Inorg. Chem. **2002**, *41*, 3218–3229

Diverse Evolution of [{$Ph_2P(CH_2)_nPPh_2$}Pt(μ-S)$_2$Pt{$Ph_2P(CH_2)_nPPh_2$}] (n = 2, 3) Metalloligands in CH_2Cl_2

Rubén Mas-Ballesté,[†] Mercè Capdevila,[†] Paul A. Champkin,[‡] William Clegg,[‡] Robert A. Coxall,[‡] Agustí Lledós,[†] Claire Mégret,[†] and Pilar González-Duarte*,[†]

Departament de Química, Universitat Autònoma de Barcelona, E-08193 Bellaterra, Barcelona, Spain, and Department of Chemistry, University of Newcastle, Newcastle upon Tyne NE1 7RU, U.K.

Received July 6, 2001

The nucleophilicity of the {Pt_2S_2} core in [{$Ph_2P(CH_2)_nPPh_2$}Pt(μ-S)$_2$Pt{$Ph_2P(CH_2)_nPPh_2$}] (n = 3, dppp (**1**); n = 2, dppe (**2**)) metalloligands toward the CH_2Cl_2 solvent has been thoroughly studied. Complex **1**, which has been obtained and characterized by X-ray diffraction, is structurally related to **2** and consists of dinuclear molecules with a hinged {Pt_2S_2} central ring. The reaction of **1** and **2** with CH_2Cl_2 has been followed by means of ^{31}P, ^{1}H, and ^{13}C NMR, electrospray ionization mass spectrometry, and X-ray data. Although both reactions proceed at different rates, the first steps are common and lead to a mixture of the corresponding mononuclear complexes [Pt{$Ph_2P(CH_2)_nPPh_2$}(S_2CH_2)], n = 3 (**7**), 2 (**8**), and [Pt{$Ph_2P(CH_2)_nPPh_2$}Cl_2], n = 3 (**9**), 2 (**10**). Theoretical calculations give support to the proposed pathway for the disintegration process of the {Pt_2S_2} ring. Only in the case of **1**, the reaction proceeds further yielding [Pt_2(dppp)$_2$\{μ-(SCH_2SCH_2S)-*S*,*S*′}]Cl_2 (**11**). To confirm the sequence of the reactions leading from **1** and **2** to the final products **9** and **11** or **8** and **10**, respectively, complexes **7**, **8**, and **11** have been synthesized and structurally characterized. Additional experiments have allowed elucidation of the reaction mechanism involved from **7** to **11**, and thus, the origin of the CH_2 groups that participate in the expansion of the $(SCH_2S)^{2-}$ ligand in **7** to afford the bridging $(SCH_2SCH_2S)^{2-}$ ligand in **11** has been established. The X-ray structure of **11** is totally unprecedented and consists of a hinged {(dppp)Pt(μ-S)$_2$Pt(dppp)} core capped by a CH_2SCH_2 fragment.

Introduction

Evolution of the chemistry of [L_2Pt(μ-S)$_2$PtL_2] as a metalloligand precursor to higher nuclearity aggregates has proceeded so rapidly since the first report of [Pt_2(PMe_2Ph)$_4$-(μ-S)$_2$] by Chatt and Mingos in 1970[1] that it appears difficult to further extend the present knowledge of the synthesis and structural aspects of the corresponding homo- and heterometallic derivatives. The recent developments in the synthesis, structures, and reactivities of sulfide-bridged aggregates with the {Pt_2S_2} core have been excellently reviewed by Fong and Hor,[2] who have made important contributions to this field.[3] The high nucleophilicity of the bridging sulfur atoms together with the flexible hinge angle between the two $Pt^{II}S_2$ planes explains the large family of derivatives based on the {Pt_2S_2} core and the varied coordination geometries about the heterometal in complexes containing the [L_2Pt-(μ-S)$_2$PtL_2] metalloligand.[4]

Despite the formidable body of structural and related data on this family of compounds, several points remained open to consideration. On one hand, the synthetic routes reported for complexes of formula [L_2Pt(μ-S)$_2$PtL_2] were not straightforward, reports on their crystal structures were scarce, and most of the sulfide-bridged aggregates containing the {Pt_2S_2} core had been achieved with PPh_3 as terminal ligand.[2,3] These observations led us to report a convenient synthesis (90% yield), monitored by means of ^{31}P NMR, for [(dppe)Pt(μ-

* Corresponding author. E-mail: Pilar.Gonzalez.Duarte@uab.es.
[†] Universitat Autònoma de Barcelona.
[‡] University of Newcastle.

(1) Chatt, J.; Mingos, D. M. P. *J. Chem. Soc. A* **1970**, 1243.
(2) Fong, S.-W. A.; Hor, T. S. A. *J. Chem. Soc., Dalton Trans*. **1999**, 639.
(3) Selected recent references: (a) Li, Z.; Loh, Z.-H.; Mok, K. F.; Hor, T. S. A. *Inorg. Chem.* **2000**, *39*, 5299. (b) Li, Z.; Xu, X.; Khoo, S. B.; Mok, K. F.; Hor, T. S. A. *J. Chem. Soc., Dalton Trans*. **2000**, 2901. (c) Liu, H.; Jiang, C.; Yeo, J. S. L.; Mok, K. F.; Liu, L. K.; Hor, T. S. A.; Yan, Y. K. *J. Organomet. Chem*. **2000**, *595*, 276. (d) Fong, S.-W. A.; Vittal, J. J.; Henderson, W.; Hor, T. S. A.; Oliver, A. G.; Rickard, C. E. F. *Chem. Commun*. **2001**, 421.
(4) (a) Capdevila, M.; Clegg, W.; González-Duarte, P.; Jarid, A.; Lledós, A. *Inorg. Chem*. **1996**, *35*, 490. (b) Aullón, G.; Ujaque, G.; Lledós, A.; Alvarez, S.; Alemany, P. *Inorg. Chem*. **1998**, *37*, 804.

10.1021/ic0107173 CCC: $22.00
Published on Web 05/17/2002

Scheme 1

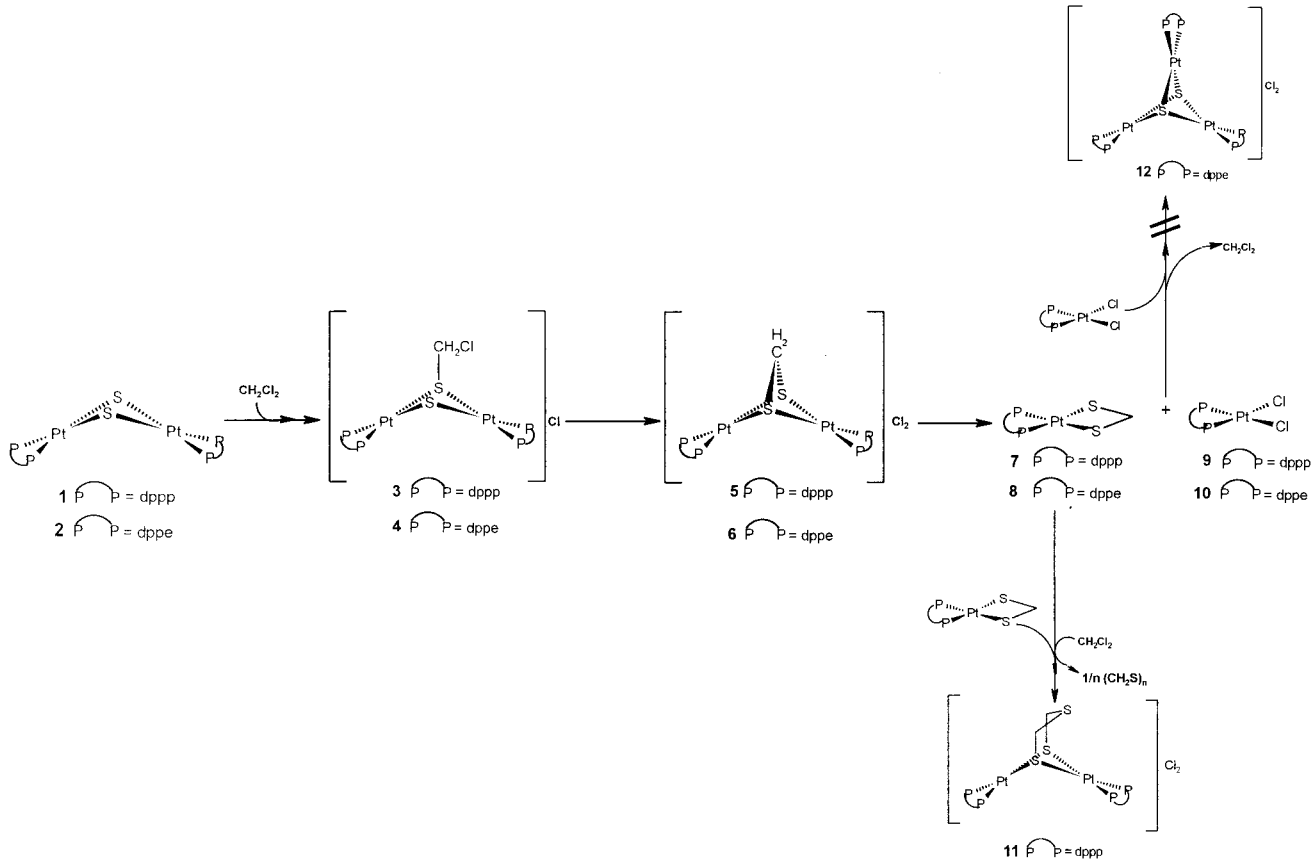

S)$_2$Pt(dppe)], its X-ray crystal structure,[5] and the synthesis and full structural characterization in the solid phase as well as in solution by multinuclear NMR of a series of pentanuclear complexes of formula [M{Pt$_2$(dppe)$_2$(μ_3-S)$_2$}$_2$], (M^{II} = Zn, Cd, Hg, Cu).[5,6] These constituted the first examples structurally characterized by X-ray diffraction where the heterometal is tetrahedrally coordinated to two [L$_2$Pt(μ-S)$_2$PtL$_2$] metalloligands.

Another question there has been insufficient information to address is the reaction pathway by which the [L$_2$Pt-(μ-S)$_2$PtL$_2$] metalloligands react with organic electrophilic agents, such as PhCH$_2$Br[1] and CH$_3$I,[7] as a consequence of the nucleophilicity of the sulfide bridges. A particular case of this well-established reaction is the surprising progression of [L$_2$Pt(μ-S)$_2$PtL$_2$] compounds when they are dissolved in CH$_2$Cl$_2$.[2] Thus, in recent years, several different species have been characterized as a result of this reaction (Table 1). The apparent dispersion of the compounds obtained, the lack of a systematic study of the reactions involved and the possible relationship between the nucleophilic character of the {Pt$_2$S$_2$} core and the nature of the terminal ligands suggested to us that this whole question deserves further analysis.

(5) Capdevila, M.; Carrasco, Y.; Clegg, W.; González-Duarte, P.; Lledós, A.; Sola, J.; Ujaque, G. *J. Chem. Soc., Chem. Commun.* **1998**, 597.
(6) Capdevila, M.; Carrasco, Y.; Clegg, W.; Coxall, R. A.; González-Duarte, P.; Lledós, A.; Ramírez, J. A. *J. Chem. Soc., Dalton Trans.* **1999**, 3103.
(7) (a) Ugo, R.; La Monica, G.; Cenini, S.; Segre, A.; Conti, F. *J. Chem. Soc. A* **1971**, 522. (b) Briant, C. E.; Gardner, C. J.; Hor, T. S. A.; Howells, N. D.; Mingos, D. M. P. *J. Chem. Soc., Dalton Trans.* **1984**, 2645.

Table 1. Complexes Obtained upon Exposure of [L$_2$Pt(μ-S)$_2$PtL$_2$] Metalloligands in CH$_2$Cl$_2$

complex	terminal ligand	experimental evidences	ref.
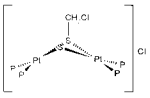	P= PPh$_3$ P$_2$= dppf [a]	NMR	8, 9
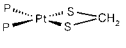	P= PMe$_2$Ph P= dppy [b]	NMR and X-ray diffraction	10, 11
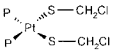	P$_2$= dppf [a] P= PPh$_3$	NMR	9, 12

[a] dppf = [FeC$_5$H$_4$PPh$_2$)$_2$]. [b] dppy = PPh$_2$(C$_5$H$_5$N).

Here we report a detailed study of the multistage pathway followed in the reaction of the [(P∩P)Pt(μ-S)$_2$Pt(P∩P)] metalloligands, where P∩P = dppe or dppp, with CH$_2$Cl$_2$, Scheme 1. On the basis of multinuclear NMR, electrospray ionization mass spectrometry (ESI MS), and X-ray crystallographic data, we show that both reactions proceed at different rates and eventually afford different products. Overall, the complexity of the reaction of the [(P∩P)Pt-(μ-S)$_2$Pt(P∩P)] metalloligands with CH$_2$Cl$_2$ explains the diversity of the compounds reported in closely related systems, Table 1, and evidences the influence of the terminal ligands on the reactivity of the {Pt(μ-S)$_2$Pt} core.

Experimental Section

Materials and Methods. All the manipulations were carried out at room temperature under an atmosphere of pure dinitrogen, and conventionally dried and degassed solvents were used throughout. These were Purex Analytical Grade from SDS. Metal complexes of formula $[PtCl_2(P\cap P)]$, P∩P = dppe or dppp, were prepared according to published methods.[13] The synthesis of [(dppe)Pt-(μ-S)$_2$Pt(dppe)] (**2**) has already been reported.[5]

Elemental analyses were performed on a Carlo-Erba CHNS EA-1108 analyzer. The microanalytical data for crystals of **11** have been omitted because they are unsatisfactory, as already found in some related phosphine platinum complexes.[14] ^{1}H, ^{13}C{^{1}H}, and ^{31}P{^{1}H} NMR spectra of the complexes **1**, **2**, and **7**−**11** and the ^{31}P{^{1}H} NMR spectrum of **11′** (**E** + **E′** in Scheme 2) were recorded from samples in $(CD_3)_2SO$ solution at room temperature using a Bruker AC250 spectrometer. ^{13}C and ^{1}H chemical shifts are relative to $SiMe_4$, and ^{31}P chemical shifts, to external 85% H_3PO_4. The ^{2}H NMR spectrum of **11′** was recorded from $(CH_3)_2SO$ solution using a Bruker AM400 spectrometer, and the ^{1}H NMR spectrum was recorded from $(CD_3)_2SO$ solution using a Bruker Avance500. The ^{31}P{^{1}H} NMR spectra of **1**, **2**, and **3** were simulated on a Pentium-200 computer using the gNMR V4.0.1 program by P. H. M. Budzelaar from Cherwell Scientific Publishing.[15]

To analyze the course of the reaction of **1** or **2** in CH_2Cl_2, a solution of 50 mg of the corresponding pure compound in 25 mL of solvent was prepared at room temperature. At different times, aliquots were taken from the solution, they were evaporated to dryness, and the ^{1}H, ^{13}C, and ^{31}P NMR spectra of a fraction of the solid residue dissolved in d_6-DMSO were recorded. Another fraction was used in order to determine the mass of the species present by means of ESI MS measurements. These were performed on a VG Quattro Micromass Instrument. Experimental conditions were as follows: 10 μL of sample was injected at 15 μL/min; capillary-counter electrode voltage, 4.5 kV; lens-counter electrode voltage, 1.0 kV; cone potential, 55 V; source temperature, 90 °C; *m*/*z* range, 300−1600. The carrier was acetonitrile for the spectra recorded during the reaction of **1**, **2**, or **7** with CH_2Cl_2 or a 1:1 mixture of acetonitrile and water containing 1% formic acid in the case of the pure **1**, **2**, **7**, **8**, and **11** complexes. ESI MS data provided evidence for the formation of **3**, **4**, and **5**.

[Pt$_2$(dppp)$_2$(μ-S)$_2$] (1). $[PtCl_2(dppp)]$ (0.20 g, 0.3 mmol) was added to a benzene solution (75 mL) of $Na_2S\cdot 9H_2O$ (0.35 g, 1.6 mmol) and the mixture stirred at room temperature for 8 h. These reaction conditions were fixed after monitoring the reaction by ^{31}P NMR, as already reported for the dppe analogue.[6] The excess $Na_2S\cdot 9H_2O$, the formed NaCl, and the $[PtCl_2(dppp)]$ which did not react were filtered off. The solvent was removed under vacuum from the filtrate to yield the product as an orange solid. Yield 84%. Anal. Calcd for $C_{54}H_{52}P_4Pt_2S_2$: C, 50.70; H, 4.10; S, 5.01. Found: C, 50.83; H, 4.29; S, 5.12. X-ray quality crystals of this compound were obtained by slow evaporation of a solution of **1** in acetone.

Table 2. Crystal Data, Data Collection, and Refinement for Complexes **1**, **7**, and **11**

	1·Me_2CO	**7**·MeCN	**11**·1.5PhMe
formula	$C_{57}H_{58}OP_4Pt_2S_2$	$C_{30}H_{35}NP_2PtS_2$	$C_{66.5}H_{68}Cl_2P_4Pt_2S_3$
fw	1337.2	730.7	1548.4
cryst size, mm^3	0.7 × 0.3 × 0.2	0.4 × 0.3 × 0.2	0.24 × 0.18 × 0.08
space group	$P2_1/c$	$P2_1/c$	$P2_1/c$
a, Å	22.025(8)	9.8365(5)	13.8539(5)
b, Å	14.753(5)	16.6498(9)	13.0377(5)
c, Å	16.502(5)	17.7108(9)	34.1386(13)
β, deg	101.470(14)	100.589(1)	91.7764(6)
V, Å^3	5255(3)	2851.2(3)	6163.3(4)
Z	4	4	4
ρ_{calcd}, g cm^{-3}	1.690	1.702	1.669
μ, cm^{-1}	55.6	52.0	48.7
$R(F)^a$ ($F^2 > 2\sigma(F^2)$)	0.0305	0.0226	0.0464
$R_w(F^2)^b$ (all data)	0.0543	0.0532	0.0982

^{a} $R(F) = \sum||F_o| - |F_c||/\sum|F_o|$. ^{b} $R_w(F^2) = [\sum[w(F_o^2 - F_c^2)^2]/\sum[w(F_o^2)^2]]^{1/2}$.

[Pt(dppp)(S$_2$CH$_2$)] (7). To a suspension of $Na_2S\cdot 9H_2O$ (0.35 g, 1.6 mmol) in benzene (50 mL) were added solid $[PtCl_2(dppp)]$ (0.10 g, 0.15 mmol) and CH_2Cl_2 (0.5 mL, 7.8 mmol) with stirring. After 24 h, the excess $Na_2S\cdot 9H_2O$ and the white solid formed, NaCl, were filtered off. The filtrate was concentrated to dryness, giving a yellow solid. Recrystallization in acetonitrile afforded a yellow crystalline solid. Yield 43%. Anal. Calcd for $C_{28}H_{28}P_2PtS_2\cdot CH_3CN$: C, 49.58; H, 4.30; N, 1.93; S, 8.82. Found: C, 48.79; H, 4.20; N, 2.22; S, 8.90. A single crystal was chosen for X-ray diffraction.

[Pt(dppe)(S$_2$CH$_2$)] (8). Using the same procedure as that indicated for complex **7**, a yellow solid was obtained from the reaction of $[PtCl_2(dppe)]$ (0.085 g, 0.1 mmol) with $Na_2S\cdot 9H_2O$ (0.175 g, 0.8 mmol) and CH_2Cl_2 (0.5 mL, 7.8 mmol) in a benzene solution (25 mL). Yield 67%. Anal. Calcd for $C_{27}H_{26}P_2PtS_2$: C, 48.28; H, 3.90; S, 9.55. Found: C, 48.03; H, 4.10; S, 10.15. Recrystallization of **8** in acetone allowed isolation of yellow crystals. Unfortunately, the diffraction data were very weak and of inferior quality compared to those of **7**, allowing only a qualitative structure analysis.

[Pt$_2$(dppp)$_2${μ-(SCH$_2$SCH$_2$S)-*S*,*S*′}]Cl$_2$ (11). A pure solid sample of **7** (0.05 g, 0.07 mmol) was added to CH_2Cl_2 (5 mL) with stirring. After several days, the solution was concentrated to dryness affording a pale yellow solid. The residue was redissolved in toluene, and the filtered solution was concentrated to yield the expected product as a pale yellow solid, which was filtered and dried. Recrystallization of **11** from toluene gave colorless crystals suitable for X-ray diffraction.

To carry out the study of the mechanism involved in the reaction from **7** to **11**, 30 mg of **7** were dissolved in 1 mL of CD_2Cl_2. By a similar procedure as that followed for **11**, 15 mg (50% yield) of **11′** were obtained. Characterization of this solid was made by multinuclear NMR spectroscopy.

X-ray Crystallographic Characterization of Complexes 1, 7, and 11. A summary of crystal data, data collection, and refinement parameters for the three structural analyses is given in Table 2. Crystals were examined on a Bruker AXS SMART CCD area-detector diffractometer with graphite-monochromated Mo Kα radiation (λ = 0.71073 Å); measurements were made at 160 K. Cell parameters were obtained from a least-squares fit on the observed setting angles of all significant intensity reflections.

(8) Gukathasan, R. R.; Morris, R. H.; Walker, A. *Can. J. Chem.* **1983**, *61*, 2490.
(9) Zhou, M.; Lam, C. F.; Mok, K. F.; Leung, P.-H.; Hor, T. S. A. *J. Organomet. Chem.* **1994**, *476*, C32.
(10) Shaver, A.; Lai, R. D.; Bird, P. H.; Wickramasinghe, W. *Can. J. Chem.* **1985**, *63*, 2555.
(11) Yam, V. W.-W.; Kok-Yan, P.; Cheung, K.-K. *J. Chem. Soc., Chem. Commun.* **1995**, 267.
(12) Zhou, M.; Leung, P.-H.; Mok, K. F.; Hor, T. S. A. *Polyhedron* **1996**, *15*, 1737.
(13) Brown, M. P.; Puddephatt, R. J.; Rashidi, M.; Seddon, K. R. *J. Chem. Soc., Dalton Trans.* **1977**, 951.
(14) Capdevila, M.; González-Duarte, P.; Foces-Foces, C.; Hernandez-Cano, F.; Martínez-Ripoll, M. *J. Chem. Soc., Dalton Trans*. **1990**, 143.
(15) Budzelaar, P. H. M. *gNMR V4.01*; Cherwell Scientific Publishing Ltd.: Oxford, UK, 1997.

Table 3. ESI MS and NMR Data for Complexes **1**−**5** and **7**−**11**

cmpd	*m*/*z*	calcd MW[a]	δP (ppm)	$^1J_{Pt-P}$ (Hz)	δH(SCH₂) (ppm)	$^3J_{Pt-H}$(SCH₂) (Hz)	δC(SCH₂) (ppm)
1	1279.7	1279.13	−0.08[b]	2615[b]			
2	1251.7	1251.18	40.5[c]	2740[c]			
3	1328.2	1328.66	P_A: 2.1[d]	Pt−P_A: 2410[d]	4.19	28	54.6
			P_B: 1.6	Pt−P_B: 3165			
4	1300.0	1300.61	P_A: 46.2	Pt−P_A: 2678	4.10	?	?
			P_B: 45.3	Pt−P_B: 3421			
5	646.7[e]	1293.21					
7	686.4	685.68	−2.25	2705	5.45	37	38.6
8	671.9	671.65	39.4	2824	5.93	34	41.9
9			−3.7	3408			
10			43.4	3610			
11	669.5[e]	1341.31	−0.14	2909	4.19		37.1

[a] Only the neutral or cationic complex species is considered. [b] ^{31}P RMN parameters from the computer simulation for **1**: $\delta P = -0.07$ ppm; $^1J_{Pt-P} = 2612$ Hz; $^2J_{Pt-Pt} = 758$ Hz; $^3J_{Pt-P} = 28$ Hz; $^4J_{P-P} = 22$ Hz. [c] From ref 6. [d] ^{31}P RMN parameters from the computer simulation for **3**: $\delta P_A = 2.0$ ppm; $\delta P_B = 1.7$ ppm; $^1J_{Pt-P(A)} = 2412$ Hz; $^1J_{Pt-P(B)} = 3164$ Hz; $^2J_{Pt-Pt} = 750$ Hz; $^3J_{Pt-P(A)} = 42$ Hz; $^3J_{Pt-P(B)} = 33$ Hz; $^4J_{P(A)-P(A)} = 21$ Hz; $^4J_{P(B)-P(B)} = 23$ Hz; $^4J_{P(A)-P(B)} = 26$ Hz. [e] $M = m/z$ ($z = 2$).

Intensities were integrated from a series of 0.3° ω rotation frames covering at least a hemisphere of reciprocal space and were corrected for absorption and other effects by semiempirical methods based on redundant and symmetry-equivalent reflections.[16]

The structures were solved by direct methods and were refined by full-matrix least-squares on all unique F^2 values, with anisotropic displacement parameters for non-hydrogen atoms and with isotropic H atoms constrained with a riding model.[17] The largest residual electron density peaks were close to Pt atoms in each case. One toluene solvent molecule in the structure of **11** is disordered over an inversion center.

The main bond distances and angles for these complexes are given in Table 5.

Computational Details. Calculations were performed with the GAUSSIAN 98 series of programs.[18] The DFT (density functional theory) was applied with the B3LYP function.[19] Effective core potentials (ECPs) were used to represent the innermost electrons of the platinum atom[20a] as well as the electron core of P, S, and Cl atoms.[20b] The basis set for the metal was that associated with the pseudopotential,[20a] with a standard double-ζ LANL2DZ contraction.[18] The basis set for the P, S, and Cl atoms was that associated with the pseudopotential,[20b] with a standard double-ζ LANL1DZ contraction[18] supplemented with a set of d-polarization functions.[21] A 6-31G basis set was used for the C and H atoms.[22] Solvent effects were taken into account by means of PCM calculations[23] using standard options of PCM and cavity keywords.[18] Free energies of solvation were calculated with CH_2Cl_2 ($\epsilon = 8.93$) as solvent, keeping the geometry optimized for the isolated species (single-point calculations). Very recently, this approach has been successfully applied to the study of bimetallic polysulfides $Cp_2Fe_2S_4$.[24]

Results and Discussion

Experimental Study of the Reaction Pathway from 1 to 9 and 11, and from 2 to 8 and 10. The first information obtained on the reaction of [(dppp)Pt(μ-S)$_2$Pt(dppp)] (**1**) in CH_2Cl_2 (Scheme 1) was the series of ^{31}P NMR spectra recorded as a function of time (Figure 1). They indicated that **1** evolved to [(dppp)Pt(μ-S)(μ-SCH$_2$Cl)Pt(dppp)]Cl (**3**), which immediately transformed into a mixture of [Pt(dppp)(S$_2$CH$_2$)] (**7**) and [Pt(dppp)Cl$_2$] (**9**). Then, while the latter remained unchanged, **7** disappeared to give rise to [Pt$_2$(dppp)$_2${μ-(SCH$_2$SCH$_2$S)-*S*,*S*′}]Cl$_2$ (**11**). However, the apparent complexity of this process together with the simultaneous presence of several species throughout the time since the exposure of **1** to CH_2Cl_2 made it necessary to obtain ^{1}H and ^{13}C NMR and ESI MS complementary data. NMR parameters and ESI-MS mass determinations for compounds **1**−**11** are shown in Table 3.

The ^{31}P NMR spectrum of **1** shows the same features as that of **2** already reported,[6] in good concordance with their similar structures in the solid phase.[5] In **1** and **2**, all the ^{31}P nuclei show the same chemical shift but are not magnetically equivalent. Interpretation of these spectra with the aid of computer simulations requires consideration of second-order effects due to $^2J_{Pt-Pt}$, $^3J_{Pt-P}$, and $^4J_{P-P}$ couplings. On the basis of ^{1}H and ^{13}C DEPT135 NMR data, it was reasonable to assume that the first species formed as a result of the

(16) Sheldrick, G. M. *SADABS*; Bruker AXS: Madison, WI, 1997.
(17) Sheldrick, G. M. *SHELXTL*, Version 5; Bruker AXS: Madison, WI, 1994.
(18) Frisch, M. J.; Trucks, G. W.; Schlegel, H. B.; Scuseria, G. E.; Robb, M. A.; Cheeseman, J. R.; Zakrzewski, V. G.; Montgomery, J. A., Jr.; Stratmann, R. E.; Burant, J. C.; Dapprich, S.; Millam, J. M.; Daniels, A. D.; Kudin, K. N.; Strain, M. C.; Farkas, O.; Tomasi, J.; Barone, V.; Cossi, M.; Cammi, R.; Mennucci, B.; Pomelli, C.; Adamo, C.; Clifford, S.; Ochterski, J.; Petersson, G. A.; Ayala, P. Y.; Cui, Q.; Morokuma, K.; Malick, D. K.; Rabuck, A. D.; Raghavachari, K.; Foresman, J. B.; Cioslowski, J.; Ortiz, J. V.; Stefanov, B. B.; Liu, G.; Liashenko, A.; Piskorz, P.; Komaromi, I.; Gomperts, R.; Martin, R. L.; Fox, D. J.; Keith, T.; Al-Laham, M. A.; Peng, C. Y.; Nanayakkara, A.; Gonzalez, C.; Challacombe, M.; Gill, P. M. W.; Johnson, B. G.; Chen, W.; Wong, M. W.; Andres, J. L.; Head-Gordon, M.; Replogle, E. S.; Pople, J. A. *Gaussian 98*, revision A.6; Gaussian, Inc.: Pittsburgh, PA, 1998.
(19) (a) Lee, C.; Yang, W.; Parr, R. G. *Phys. Rev.* **1988**, *B37*, 785. (b) Becke, A. D. *J. Chem. Phys.* **1993**, *98*, 5648. (c) Stephens, P. J.; Delvin, F. J.; Chabalowski, C. F.; Frisch, M. J. *J. Phys. Chem.* **1994**, *98*, 11623.
(20) (a) Hay, P. J.; Wadt, W. R. *J. Chem. Phys.* **1985**, *82*, 299. (b) Wadt, W. R.; Hay, P. J. *J. Chem. Phys.* **1985**, *82*, 284.
(21) Höllwarth, A.; Böhme, M.; Dapprich, S.; Ehlers, A. W.; Gobbi, A.; Jonas, V.; Köhler, K. F.; Stegman, R.; Veldkamp, A.; Frenking, G. *Chem. Phys. Lett.* **1993**, *208*, 237.
(22) Hehre, W. J.; Ditchfield, R.; Pople, J. A. *J. Chem. Phys.* **1972**, *56*, 2257.
(23) (a) Tomasi, J.; Persico, M. *Chem. Rev.* **1994**, *94*, 2027. (b) Amovilli, C.; Barone, V.; Cammi, R.; Cancès, E.; Cossi, M.; Mennucci, B.; Pomelli, C. S.; Tomasi, J. *Adv. Quantum Chem.* **1998**, *32*, 227.
(24) Blasco, S.; Demachy, I.; Jean, Y.; Lledós, A. *New J. Chem.* **2001**, *25*, 611.

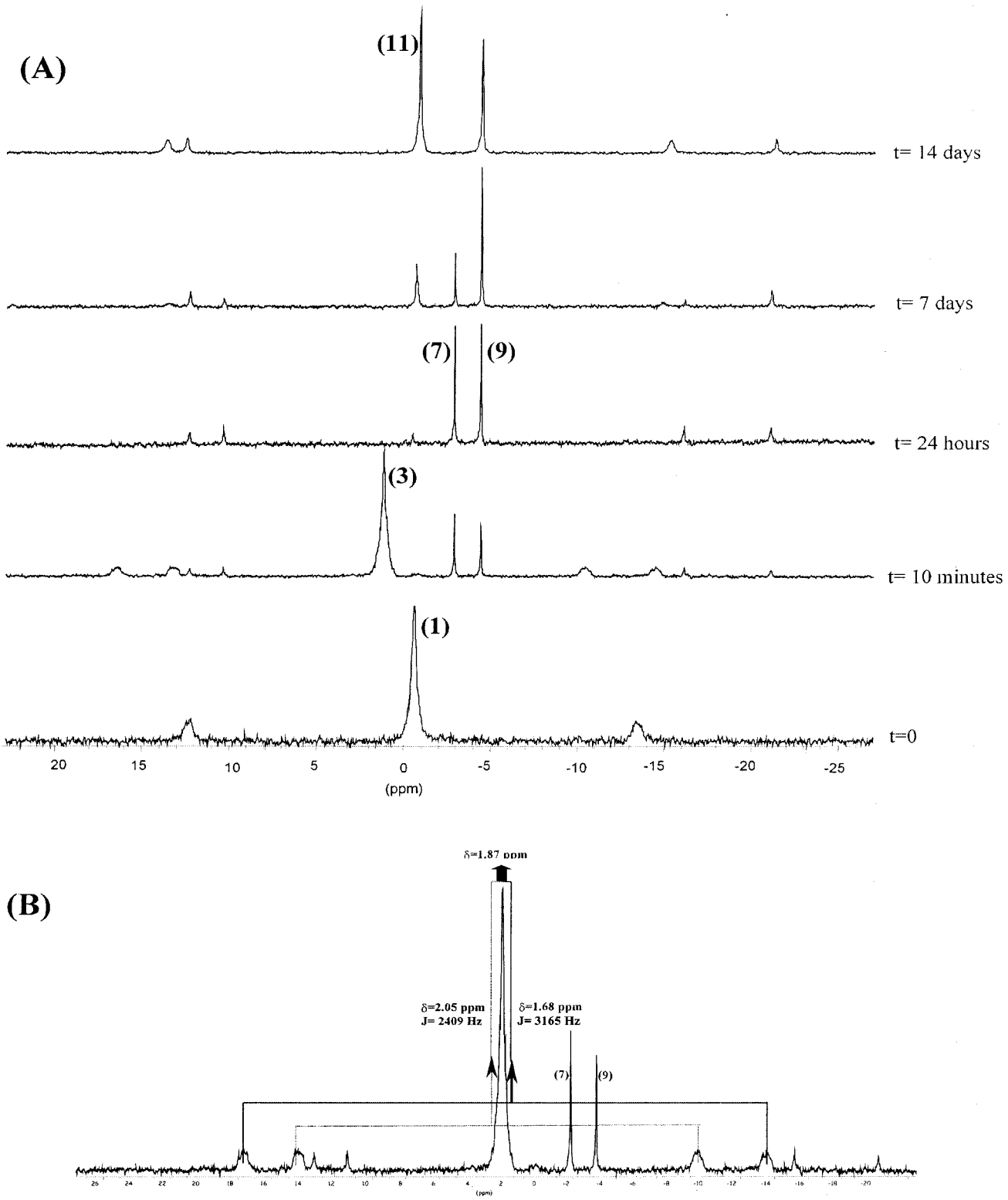

Figure 1. (A) Progression of **1** in CH_2Cl_2 as a function of time monitored by $^{31}P\{^1H\}$ NMR. Spectra of the different aliquots were recorded in d_6-DMSO. (B) Analysis of the $^{31}P\{^1H\}$ NMR spectra of **3**.

nucleophilic attack of **1** to CH_2Cl_2 solvent involved the binding of one CH_2Cl fragment to a sulfide bridge while the remaining chloride behaved as a counterion. ESI MS data clearly confirmed that the new species, **3**, could be formulated as [**1**.CH_2Cl]Cl (molecular weight of the cation of **3**, 1328.66). Its ^{31}P NMR spectrum consisting of only one signal with four satellites was indicative of the asymmetry of **3**, thus corroborating the attack of only one CH_2Cl_2 molecule. This spectrum, which is comparable to that reported for the analogue with PPh_3 as terminal ligand,[8] could be interpreted by considering that the two chemically nonequivalent ^{31}P nuclei in **3** show a very close chemical shift but different $^1J_{Pt-P}$ values. This difference could be attributed to the different nature and thus trans influence of the bridging S^{2-}

or SCH_2Cl^- ligands. The chemical shift values δP_A and δP_B were taken as the midpoint between the two satellites corresponding to the $^1J_{Pt-P(A)}$ and $^1J_{Pt-P(B)}$ couplings, respectively (Figure 1). These δP_A, δP_B, $^1J_{Pt-P(A)}$, and $^1J_{Pt-P(B)}$ values were used for a full computer simulation, which allowed a good match with the experimental spectrum.

ESI MS determinations not only led to the identification of $[(dppp)Pt(\mu\text{-}S_2CH_2)Pt(dppp)]Cl_2$, **5** (molecular weight of its cation, 1293.21), which was undetected by NMR measurements run in parallel, but also evidenced the coexistence in solution of **1**, **3**, **5**, and **7**. The ^{31}P NMR spectra of the subsequent species formed, **7** and **9**, were consistent with a first-order analysis and showed only one chemical shift for each complex. This indicated that all the respective phosphorus nuclei were chemically and magnetically equivalent in solution. Further reaction of **7** affords **11**. On the basis of the whole set of the spectroscopic data obtained for **11** (ESI MS, ^1H, ^{13}C and ^{31}P NMR), it was possible to determine its structure, which would otherwise involve a second-order ^{31}P NMR spectrum. However, in this complex, the second-order effects appear to be small, and the ^{31}P NMR spectrum allows a first-order analysis. In addition, the only chemical shift that is observed in this spectrum at room temperature indicates a fast flipping of the thioether sulfur atom. ^1H and ^{13}C NMR data suggested that **7** and **11** included $(SCH_2S)^{2-}$ or $(SCH_2SCH_2S)^{2-}$ groups, respectively. The observation that the ^{31}P NMR parameters for **9** were coincident with those of the precursor of **1** led to its identification as the mononuclear $[Pt(dppp)Cl_2]$ species.[13,25]

Analogous to **1**, the reaction of $[(dppe)Pt(\mu\text{-}S)_2Pt(dppe)]$ (**2**) with CH_2Cl_2 (Scheme 1) was followed by means of ^{31}P NMR spectra recorded as a function of time (Figure 2) and additional ^1H and ^{13}C NMR data and ESI MS measurements. The synthesis, X-ray structure, and NMR parameters of **2** have already been reported.[5,6] The subsequent ^{31}P NMR spectra evidenced that **2** afforded $[(dppe)Pt(\mu\text{-}S)(\mu\text{-}SCH_2Cl)Pt(dppe)]Cl$ (**4**), which transformed into a mixture of $[Pt(dppe)(S_2CH_2)]$ (**8**) and $[Pt(dppe)Cl_2]$ (**10**). Complexes **8** and **10** do not react further even if they are mixed at a 1:2 mole ratio, which is the appropriate stoichiometric molar ratio to obtain $[Pt_3(\mu_3\text{-}S)_2(dppe)_3]Cl_2$, **12**, already reported.[6] This complex is obtained from a solution of **2** in either CH_2Cl_2 or $CHCl_3$ containing traces of HCl.

Unlike **3**, the ^{31}P NMR spectrum of **4** showed two different chemical shifts corresponding to two chemically inequivalent phosphorus atoms, as already reported for a closely related species containing dppf, $[Fe(C_5H_4PPh_2)_2]$, instead of dppe as terminal ligand.[9] The ^{31}P NMR spectrum allowed determination of the coupling constants involving not only P−Pt ($^1J_{Pt-P(A)}$, $^1J_{Pt-P(B)}$) but also P−P ($^4J_{P(A)-P(B)}$) nuclei, as shown in Table 3. However, at room temperature, the conversion from **2** to **8** and **10** occurred in 2 h and thus hampered recording the ^{13}C NMR spectrum of **4** and determining neither the mass nor the NMR spectral features of the possible intermediate species $[(dppe)Pt(\mu\text{-}S_2CH_2)Pt(dppe)]Cl_2$ (**6**). While the ^{31}P NMR parameters for **10** coincided with those of $[Pt(dppe)Cl_2]$, already known as a precursor of **2**, complex **8** could be fully characterized as indicated later. Analogously to complexes **7** and **9**, the ^{31}P NMR spectra of **8** and **10** were consistent with a first-order analysis.

Overall, the first stages of the reaction of **1** or **2** with CH_2Cl_2 proceed at different rates but follow a common pathway, independent of the diphosphine nature, to give a mixture of two mononuclear complexes **7** and **9** or **8** and **10**. However, only in the case of dppp, the reaction does not stop at this point, but there is a second electrophilic attack of CH_2Cl_2 on the thiolate sulfur of **7** to afford the final unprecedented complex **11**. These results indicate that dppp confers a greater nucleophilicity to the sulfur atoms and are consistent with the information obtained by theoretical calculations. The proposed pathway is corroborated by the X-ray structures of **1**, **7**, and **11** (**8** only a qualitative analysis), which are in good concordance with NMR data in solution, and by the crystal structures of **2** and **12** previously reported.[5,6]

Theoretical Study of the Pathway from Bimetallic (1, 2) to Mononuclear Complexes (7, 9 and 8, 10). We have performed DFT calculations in order to determine the structural features of the intermediates and to obtain an energetic picture of the process. In the calculations we have modeled dppp and dppe real ligands by $H_2P(CH_2)_3PH_2$ (dhpp) and $H_2P(CH_2)_2PH_2$ (dhpe), respectively. Thus, the different species are labeled with the same number as the parent compound but with an additional t. Their main geometric parameters are collected in Table 4. The calculated structures agree with the analogous products structurally characterized in this work and with other related complexes reported in the literature.[7b,26−29]

The analysis of the NPA (natural population analysis) charges indicates that the sulfides in the dhpp containing compounds have a slightly more negative charge than those with dhpe. This is a consequence of the greater positive charge supported by the dhpp ligand. Thus, sulfides in **1t** appear to be more nucleophilic than in **2t**. The same feature has been found for all the species from **1t** to **7t** if compared with those from **2t** to **8t**.

The changes in the PPtP angle for both bidentate ligands along the reaction pathway deserve further analysis. Data in Table 4 show that the changes on the PPtP angle for the dhpe ligands are small (from 85.0° in **6t** to 88.4° in **10t**) but substantial in the case of dhpp (from 91.4° in **5t** to 98.5° in **9t**). Moreover, PPtP angles in dhpp are always closer to the values found for unidentate, unconstrained systems. As a consequence, dhpp appears to be more flexible, and the corresponding complexes less strained than those with dhpe. This fact may be the origin of the observed greater reactivity

(25) (a) Robertson, G. B.; Wickramasinghe, W. A. *Acta Crystallogr., Sect. C* **1987**, *43*, 1694. (b) Farrar, D. H.; Ferguson, G. *J. Crystallogr. Spectrosc. Res.* **1982**, *12*, 465.

(26) Bos, W.; Bour, J. J.; Schlebos, P. P. J.; Hageman, P.; Bosman, W. P.; Smits, J. M. M.; van Wietmarschen, J. A. C.; Beurskens, P. T. *Inorg. Chim. Acta* **1986**, *119*, 141.

(27) Forniés-Càmer, J.; Masdeu-Bultó, A. M.; Claver, C.; Cardir, C. J. *Inorg. Chem.* **1998**, *37*, 2626.

(28) Masdeu-Bultó, A. M.; Ruiz, A.; Castillón S.; Claver, C.; Hitchcook, P. B.; Chaloner, P. A.; Bo, C.; Poblet, J. M.; Sarasa, P. *J. Chem. Soc., Dalton Trans.* **1993**, 2689.

(29) Elduque, A.; Finestra, C.; López, J. A.; Lahoz, F. J.; Merchán, F.; Oro, L. A.; Pinillos, M. T. *Inorg. Chem.* **1998**, *37*, 824.

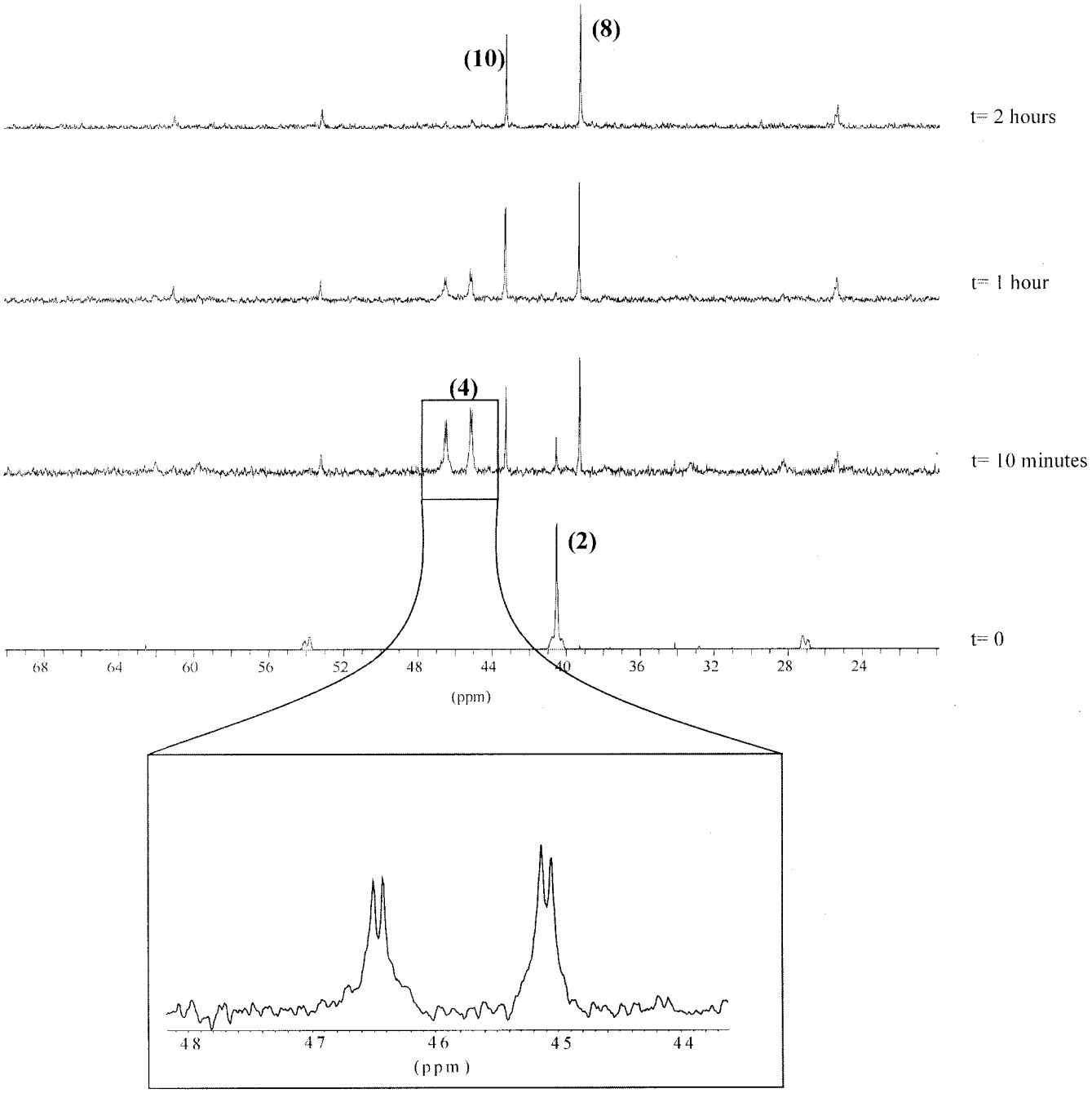

Figure 2. Progression of **2** in CH_2Cl_2 as a function of time monitored by $^{31}P\{^1H\}$ NMR. Spectra of the different aliquots were recorded in d_6-DMSO.

of the dppe containing species compared to those containing dppp. The influence of the bite angle of diphosphine ligands on the stability and catalytic behavior of metal complexes has been reviewed recently.[30]

Moreover, we have calculated the thermodynamics of the different steps of the reaction of **1t** or **2t** with dichloromethane by means of the polarizable continuum model (PCM).[23] If taking **1t** + CH_2Cl_2 and **2t** + CH_2Cl_2 as the zero of energy, the first intermediates, (**3t** + Cl^-) and (**4t** + Cl^-), are found 0.5 and 1.6 kcal/mol, respectively, above the corresponding reactants, whereas the second intermedi-

(30) Dierkes, P.; van Leeuwen, P. W. N. M. *J. Chem. Soc., Dalton Trans.* **1999**, 1519.

Table 4. Most Important Geometric Parameters[a] of the Optimized Structures **1t**−**10t**

structure	Pt−S	Pt−P	Pt···Pt	S···S	Pt−S−Pt	S−Pt−S	θ^b	P−Pt−P
1t	2.406	2.293	3.286	3.228	86.1	84.2	147.7	95.8
2t	2.399	2.299	3.301	3.216	87.0	84.2	148.9	86.6
3t	2.392	2.289	3.386	3.226	90.0	83.4	138.4	93.6
	2.458	2.336			87.1			
4t	2.400	2.282	3.331	3.087	87.9	79.3	126.9	86.0
	2.438	2.335			86.2			
5t	2.476	2.317	3.260	2.840	82.3	70.0	106.9	91.4
6t	2.470	2.318	3.251	2.842	82.3	70.2	107.1	85.0
7t	2.380	2.313		2.933		76.1		92.8
8t	2.376	2.317		2.928		76.1		85.6
9t		2.257						98.5
10t		2.253						88.4

[a] Distances in angstroms; angles in degrees. [b] Dihedral angle between the two PtS_2 planes.

ates, (**5t** + 2Cl$^-$) and (**6t** + 2Cl$^-$), lie 43.7 and 44.4 kcal/mol, respectively, above the reactants. Monometallic complexes are considerably stabilized: 27.2 kcal/mol (**7t** + **9t**) and 26.5 kcal/mol (**8t** + **10t**) below the reactants. ΔG values obtained for the second intermediates (more than 40 kcl/mol) are hardly compatible with their experimental detection at room temperature. However, the numerical values of the relative energies in solution of species differently charged (0 for the reactants, +1 and −1 for the first intermediate, and +2 and −2 for the second one) can only be given a semiquantitative significance. Calculations with inclusion of solvent effects cannot be given the same accuracy as those in the gas phase. When using the continuum model for the solvent, as in the PCM method, energies are dependent on the atomic radii used to define the cavity. This is especially important for charged species of small size as the Cl$^-$ anion. Even though this model hinders a quantitative determination of the energies of the charged species, the reaction profile obtained allows the following conclusions: (i) The driving force for the reaction is the greater stability of the two mononuclear compounds, **7t** and **9t** or **8t** and **10t**, with respect to the corresponding reactants, **1t** or **2t**, by more than 25 kcal/mol. (ii) The stabilities of the two intermediates in each of both reaction pathways are manifestly different. Whereas the first intermediate has almost the same free energy as the initial species, the second one appears as significantly more unstable. Thus, the formation of the second intermediate must be the rate-limiting step for the process.

Study of the Reaction Mechanism from 7 to 11. The synthesis of **11** from **7** allowed characterization of the former by X-ray, mass measurements, and corresponding NMR parameters in solution (Table 3). The stoichiometric molar ratio of **7** to CH_2Cl_2 in the reaction leading to **11** is 2:1. This fully confirmed that the molar ratio of **9** to **11** in the final solution obtained upon exposure of **1** in CH_2Cl_2 is 2:1, as observed by NMR data. Complex **7** is stable in acetonitrile, acetone, and methanol solvents even under open atmosphere. However, upon exposure of **7** to CH_2Cl_2, it converts to the final complex, **11**. On one hand, the complete characterization of **7** allowed confirmation of its existence as an intermediate species in the reaction of **1** with CH_2Cl_2 to give **9** and **11** (Scheme 1). On the other, the direct synthesis of **11** by reacting **7** with CH_2Cl_2 evidenced its involvement in this reaction. This finding, and comparison of the structures of **7** and **11**, raises the question of the source of the CH_2 groups that participate in the expansion of the $(SCH_2S)^{2-}$ ligand in **7** to afford the bridging $(SCH_2SCH_2S)^{2-}$ ligand in **11**. On the basis of all these data, we thought that replacement of CH_2Cl_2 by CD_2Cl_2 in the synthesis of **11** from **7** could cast light on the origin of these CH_2 groups as well as the mechanism involved in this reaction.

The reaction of **7** with CD_2Cl_2 was carried out by an analogous procedure to that followed for the synthesis of **11**, and the solid obtained, **11′**, was analyzed by means of the corresponding ^{1}H, ^{2}H, and ^{31}P NMR spectra. The ^{31}P NMR parameters for **11′** were coincident with those of **11** (Table 3), thus confirming that the same reaction had taken place. However, the comparison of the ^{1}H NMR spectra of **11′** and **11** indicated that the signal at 4.2 ppm, which is due to the protons of the $(SCH_2SCH_2S)^{2-}$ ligand, decreased by about 25% if the synthesis was run in CD_2Cl_2 instead of CH_2Cl_2. Also, in the ^{2}H NMR spectrum, there was only one signal at 4.3 ppm, thus indicating the insertion of the CD_2 group in the bridging ligand. These data showed that one-fourth of the protons in the $(SCH_2SCH_2S)^{2-}$ ligand had been replaced by deuterium. This allows the conclusion that for each pair of **11** formed, one species contains $(SCH_2SCH_2S)^{2-}$ and the other $(SCH_2SCD_2S)^{2-}$ as bridging ligands. Or, when the reaction is run in CH_2Cl_2 to give $[Pt_2(dppp)_2\{\mu$-(SCH_2SCH_2S)-$S,S'\}]Cl_2$ (**11**), one-fourth of the CH_2 groups of the bridging ligand comes from the CH_2Cl_2 solvent and three-fourths from the starting material, [Pt(dppp)(S_2CH_2)] (**7**). All these observations are consistent with the reaction mechanism proposed in Scheme 2.

Accordingly, the first step in the reaction of **7** with CD_2Cl_2 to give **11′**, which comprises species **E** and **E′**, involves the electrophilic attack of a CD_2Cl_2 molecule on one sulfur atom of the dithiolate $(SCH_2S)^{2-}$ ligand in **7**. Then, cleavage of the {PtS_2C} ring in the intermediate species **A** yields a mononuclear species **B**. This includes two $(SCX_2Cl)^-$ terminal ligands, one with X = H and the other with X = D. Although **B** has not been detected in this work, analogues with PPh_3[9] and dppf[12] have been reported previously. Both $(SCX_2Cl)^-$ (X = H or D) groups in **B** are capable of carrying out an electrophilic attack on a second molecule of **7**, but only if this is done by $(SCD_2Cl)^-$ will the CD_2 fragment from the initial CD_2Cl_2 molecule be inserted into the final complex. Thus, the attack of **B** on **7** gives rise to the intermediate species **C** and **C′** where the formation of the $(SCH_2SCX_2S)^{2-}$ (X = H, D) ligand is already apparent. The loss of the SCX_2 fragment, which can afford possible oligomeric forms,[31] triggers formation of the intermediate **D** and **D′** species. The former was detected by ESI MS in the reaction of **7** with the CH_2Cl_2 solvent. An internal rearrangement of the Pt−S bonds in **D** and **D′** yields the final species **E** and **E′**, where the $(SCH_2SCX_2S)^{2-}$ ligand bridges two {Pt(dppp)} units. Overall, the proposed mechanism (Scheme 2) accounts for the inherent ability of **7** to react with the CH_2Cl_2 solvent and gives an insight into the source of the CH_2 groups, which give rise to the $(SCH_2SCH_2S)^{2-}$ ligand in the unprecedented complex **11**.

The fact that none of the intermediate species involved in the reaction mechanism is observed by ^{31}P NMR suggests that the evolution from **7** to **A** is the rate determining step. To confirm this assumption, the reaction of **7** at different concentrations in CH_2Cl_2 was monitored by ^{31}P NMR. These data were in good agreement with a pseudo-first-order rate law, and the calculated rate constant (9.8×10^{-3} h^{-1}) was independent of the initial concentration of **7**.

Molecular Structures. The crystal structure of complex **1** consists of neutral dinuclear [(dppp)Pt(μ-$S)_2$Pt(dppp)] species devoid of crystallographic symmetry elements, and acetone solvent molecules. Both types of molecules have only

(31) Schmidt, M.; Weissflog, E. *Angew. Chem., Int. Ed. Engl.* **1977**, *17*, 51.

Scheme 2

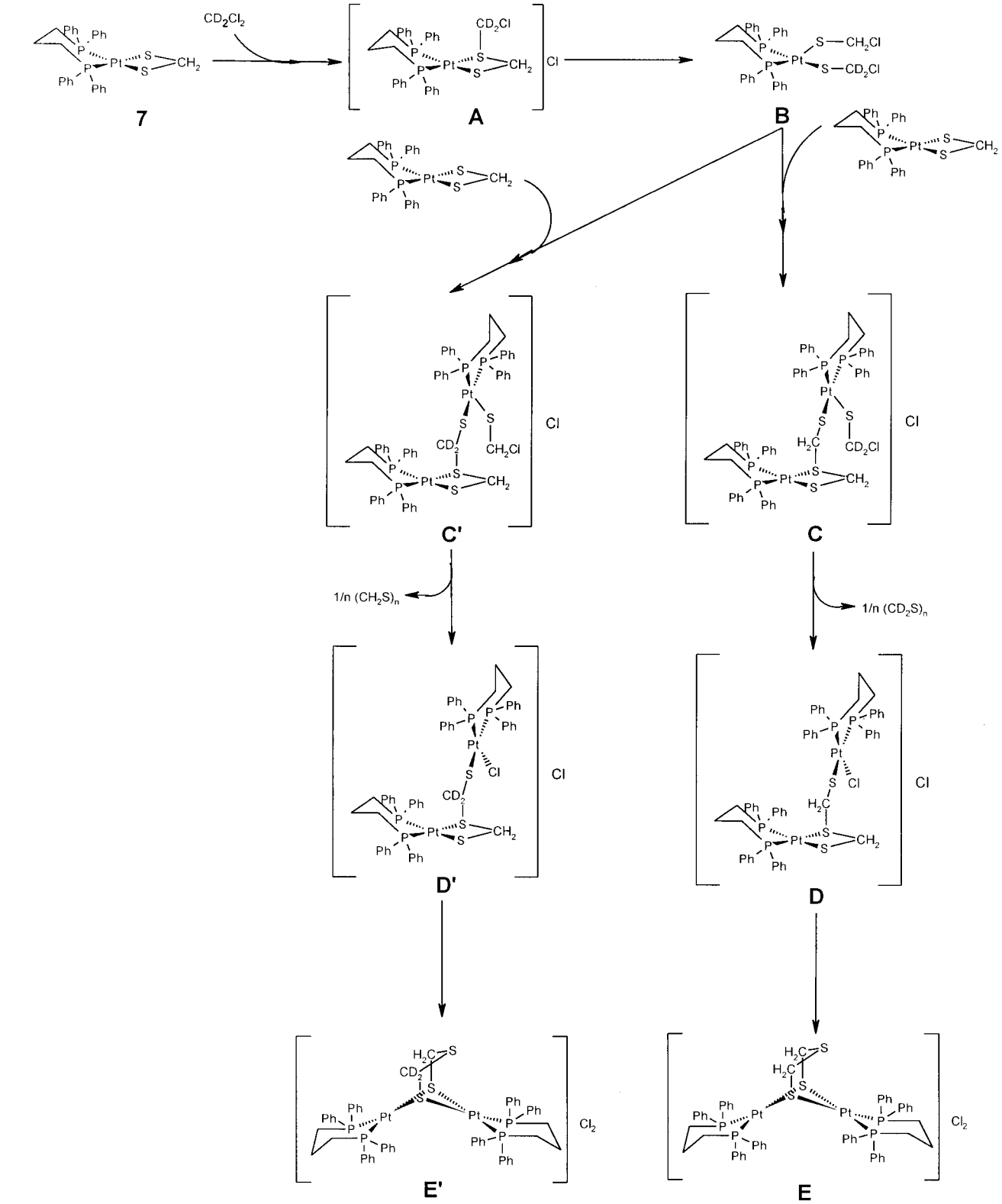

normal van der Waals interactions. Main geometric parameters for **1** (Figure 3) are given in Table 5. Each molecule shows a hinged $\{Pt_2S_2\}$ central ring, dihedral angle $\theta = 134.8°$, with the two platinum atoms bridged by two sulfide anions, coordination being completed by chelating dppp ligands. Ignoring the phenyl rings and the H atoms of the aliphatic carbon chains, the idealized symmetry of the $\{C_3P_2Pt(\mu\text{-}S)_2PtP_2C_3\}$ core is C_{2v}. It can be considered as formed by three rings, the central $\{Pt_2S_2\}$ one fused to two other PtP_2C_3, which give rise to a butterfly structural type. Both PtP_2C_3 rings show a distorted chair conformation. The geometries at the individual Pt sites are approximately square planar, deviations from planarity being less than 0.08 Å, and the Pt−S and Pt−P bond distances agree well with those

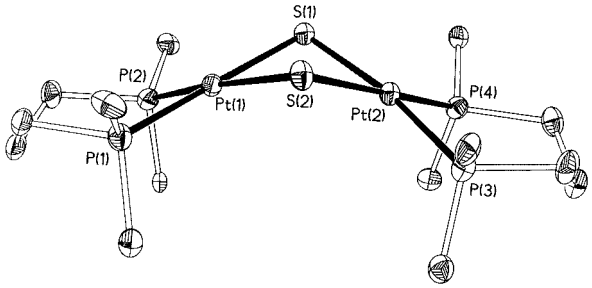

Figure 3. Molecular structure of complex **1** with key atoms labeled and with 50% probability ellipsoids. H atoms, phenyl rings, and the acetone solvent molecule are omitted.

Table 5. Selected Bond Lengths (Å) and Angles (deg) for Complexes **1**, **7**, and **11**

	Complex **1**		
Pt(1)−S(1)	2.3505(13)	Pt(2)−S(1)	2.3318(14)
Pt(1)−S(2)	2.3392(14)	Pt(2)−S(2)	2.3379(14)
Pt(1)−P(1)	2.2704(14)	Pt(2)−P(3)	2.2342(15)
Pt(1)−P(2)	2.2566(15)	Pt(2)−P(4)	2.2546(15)
S(1)−Pt(1)−S(2)	82.80(5)	S(1)−Pt(2)−S(2)	83.24(5)
P(1)−Pt(1)−P(2)	94.77(5)	P(3)−Pt(2)−P(4)	94.59(5)
Pt(1)−S(1)−Pt(2)	87.40(4)	Pt(1)−S(2)−Pt(2)	87.52(4)
	Complex **7**		
Pt(1)−S(1)	2.3214(8)	Pt(1)−S(2)	2.3281(8)
Pt(1)−P(1)	2.2596(8)	Pt(1)−P(2)	2.2558(8)
S(1)−C(30)	1.840(4)	S(2)−C(30)	1.842(4)
S(1)−Pt(1)−S(2)	76.85(3)	P(1)−Pt(1)−P(2)	92.18(3)
Pt(1)−S(1)−C(30)	89.96(12)	Pt(1)−S(2)−C(30)	89.70(11)
S(1)−C(30)−S(2)	103.36(17)		
	Complex **11**		
Pt(1)−S(1)	2.3693(14)	Pt(2)−S(1)	2.3688(14)
Pt(1)−S(2)	2.3791(14)	Pt(2)−S(2)	2.3850(14)
Pt(1)−P(1)	2.2697(16)	Pt(2)−P(3)	2.2738(15)
Pt(1)−P(2)	2.2710(15)	Pt(2)−P(4)	2.2702(14)
S(1)−C(1)	1.843(6)	S(2)−C(2)	1.854(6)
S(3)−C(1)	1.797(7)	S(3)−C(2)	1.783(6)
S(1)−Pt(1)−S(2)	82.56(5)	S(1)−Pt(2)−S(2)	82.45(5)
P(1)−Pt(1)−P(2)	90.44(6)	P(3)−Pt(2)−P(4)	92.39(5)
Pt(1)−S(1)−Pt(2)	86.94(5)	Pt(1)−S(2)−Pt(2)	86.35(5)
Pt(1)−S(1)−C(1)	102.0(2)	Pt(2)−S(1)−C(1)	106.2(2)
Pt(1)−S(2)−C(2)	101.4(2)	Pt(2)−S(2)−C(2)	106.6(2)
S(1)−C(1)−S(3)	117.9(3)	S(2)−C(2)−S(3)	117.2(3)
C(1)−S(3)−C(2)	102.0(3)		

found in dppe analogue **2**.[5] Considering the average values of the angles about the Pt atoms, the more important deviations from the ideal value correspond to P−Pt−P (94.6°) and S−Pt−S (83.0°).

The very few structurally characterized examples with a similar core to that of **1** are the $[Pt_2(dppy)_2(\mu\text{-}S)_2]$ (dppy = 2-diphenylphosphinopyridine)[11] and $[Pt_2(dppe)_2\mu\text{-}S)_2]$ (**2**)[5] complexes and the incompletely determined X-ray structure of $[Pt_2(PMe_2Ph)_4(\mu\text{-}S)_2]$.[1] Comparison of their main geometric parameters (Table 6) indicates that the most significant difference lies in the dihedral angle between the two PtS_2 planes and that a decrease in this angle entails a concomitant shortening of the Pt···Pt and smaller changes in the S···S distances.

Complexes **7** and **8** are structurally related as they both consist of mononuclear $[Pt(P\cap P)(S_2CH_2)]$ (P∩P = dppp (**7**) (Figure 4) or dppe (**8**) discrete molecules devoid of crystallographic symmetry elements. In the case of **7**, there is one

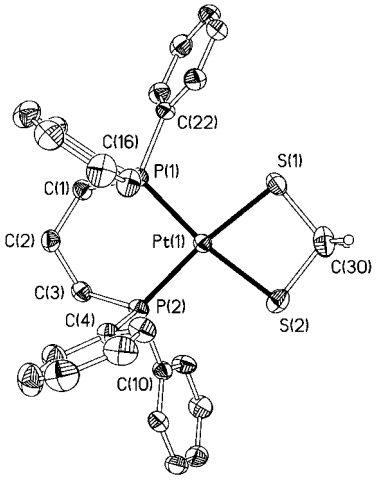

Figure 4. Molecular structure of complex **7** with key atoms labeled and with 50% probability ellipsoids. H atoms and the acetonitrile solvent molecule are omitted.

CH_3CN molecule in each formula unit. The listing of the main geometric parameters for **7** appears in Table 5. The structure can be considered as formed by two fused rings that share a platinum atom. The four-membered PtS_2C ring, which includes the chelating $[SCH_2S]^{2-}$ ligand, is essentially planar, deviations from planarity being less than 0.03 Å. The C_3P_2Pt ring includes six atoms and shows a chair conformation. The platinum atom has square planar coordination, distorted by a significant reduction of the S−Pt−S angle (76.8°) from ideal 90°, and by a twist of 5.0° between the PtS_2 and PtP_2 planes. The bite angle of the diphosphine ligand, 92.1°, dictates the values of the remaining P−Pt−S angles about the platinum atom. The structure of **8**, established qualitatively from a crystal of inferior quality, is similar in its major aspects, having one fewer C atom in the chelate ring.

Complexes of general formula $[L_2Pt(S_2CH_2)]$ with similar structure to **7** and **8** amount to only two examples, $[Pt(PMe_2Ph)_2(S_2CH_2)]$[10] and $[Pt(dppy)_2(S_2CH_2)]$,[11] both with unidentate phosphine ligands. Comparison of these complexes shows remarkable similarities, and particularly, the geometric features of their PtS_2C rings are practically identical (Table 6). Obviously, the structures differ in the P−Pt−P angles, which range from 92.2° to 100.6° (leaving out the smaller angle in **8**), but these differences have no apparent effect on the structural parameters involving the neighboring PtS_2C ring. Concerning the Pt(P∩P) moieties, their geometric features are in good concordance with those observed in **1** and **2**, respectively, as well as in $[Pt(dppp)Cl_2]$ and $[Pt(dppe)Cl_2]$ complexes known[13,25] and related species.[30]

The structure of **11** is totally unprecedented (Figure 5) and consists of dinuclear $[(dppp)Pt(\mu\text{-}SCH_2SCH_2S)Pt(dppp)]^{2+}$ cations and Cl^- counterions, together with toluene solvent molecules. Selected bond angles and distances are given in Table 5. The cation has approximate mirror symmetry. It can be described as formed by a $\{(dppp)Pt(\mu\text{-}S)_2Pt(dppp)\}$ core capped by a CH_2SCH_2 fragment, which lowers the approximate core symmetry from C_{2v} to C_s. The core shows a hinged Pt_2S_2 central ring with the two platinum atoms bridged by two thiolate sulfurs, coordination being completed

Table 6. Main Geometric Parameters[a] of the $\{Pt_2S_2\}$ and $\{PtS_2C\}$ Fragments in Structurally Characterized Complexes

complex	Pt−S	Pt−P	C−S	S−C−S	Pt···Pt	S···S	Pt−S−Pt	S−Pt−S	θ[b]	P−Pt−P	ref
$[Pt_2(dppy)_4(\mu\text{-}S)_2]$	2.33	2.28			3.55	3.01	99.6	80.4	180	102.9	11
$[Pt_2(dppe)_2(\mu\text{-}S)_2]$ (**2**)	2.35	2.24			3.29	3.13	88.9	83.7	140.2	86.2	5
$[Pt_2(dppp)_2(\mu\text{-}S)_2]$ (**1**)	2.34	2.25			3.23	3.10	87.5	83.0	134.8	94.7	*c*
$[Pt_2(PMe_2Ph)_4(\mu\text{-}S)_2]$[d]	2.34	2.26			3.17		85.5	81.6	121		1
$[Pt(dppy)_2(S_2CH_2)]$	2.31	2.27	1.82	103.0				76.2		100.6	11
$[Pt(PMe_2Ph)_2(S_2CH_2)]$	2.30	2.25	1.83	102.1				76.1		94.3	10
$[Pt(dppp)(S_2CH_2)]$ (**7**)	2.32	2.26	1.84	103.4				76.9		92.2	*c*
$[Pt(dppe)(S_2CH_2)]$ (**8**)[d]	2.32	2.27	1.84	102.0				76.2		85.4	*c*

[a] Distances in angstroms; angles in degrees. [b] Dihedral angle between the two PtS_2 planes. [c] This work. [d] Only preliminary crystallographic data.

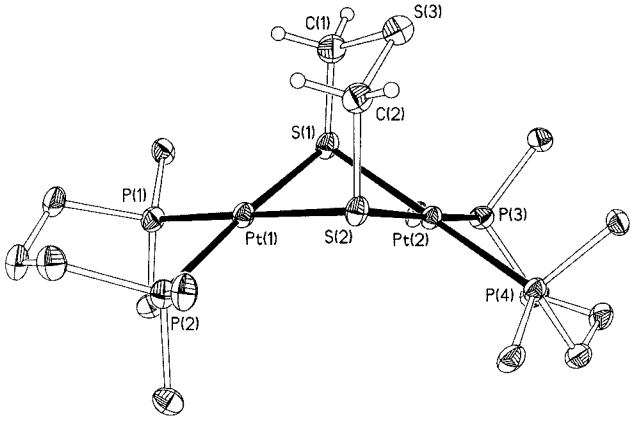

Figure 5. Structure of the cation of complex **11** with key atoms labeled and with 50% probability ellipsoids. H atoms, chloride anions, phenyl rings, and toluene solvent molecules are omitted.

by chelating dppp ligands. The dihedral angle between PtS_2 planes, $\theta = 131.7°$, is smaller than that found in the parent $[(dppp)Pt(\mu\text{-}S)_2Pt(dppp)]$ complex **1** ($\theta = 134.8°$), this reduction being less significant than that experienced by the dppe analogue **2** when acting as a metalloligand.[6] The geometries at the individual Pt sites are essentially square planar, the main distortions being due to the reduction of the S−Pt−S angles from ideal 90° (average 82.5°), and by a twist of 3.6° between the $Pt(1)S_2$ and $Pt(1)P_2$ planes and of 1.3° between $Pt(2)S_2$ and $Pt(2)P_2$. The bite angle of the diphosphine ligand involving Pt(1) (90.4°) and Pt(2) (92.4°) compares well with those found in the parent complex (**1**).

The capping CH_2SCH_2 unit can be considered within the bridging $[SCH_2SCH_2S]^{2-}$ ligand, which, according to the angles about S(1) [Pt(1)−S(1)−C(1) 102.0°; Pt(1)−S(2)−C(2) 101.4°] and S(2) [Pt(2)−S(1)−C(1) 106.2°; Pt(2)−S(2)−C(2) 106.6°], is slightly tilted toward Pt(1) while the thioether S(3) atom is clearly oriented toward Pt(2), the C(1)−S(3)−C(2) angle being 102.0°.

The main novelty of this complex is that no other structure containing the $(SCH_2SCH_2S)^{2-}$ species either as a terminal or bridging ligand has ever been reported. Also, to our knowledge, no dinuclear homometallic platinum complexes with S∩S bridging units have been characterized crystallographically. The closest examples found in the literature are the heterobimetallic bridged dithiolate platinum−rhodium complexes of general formula $[(P-P)Pt\{\mu\text{-}(S-S)\}Rh(COD)]$, where P−P = $(PPh_3)_2$ and S−S = $S(CH_2)_nS$ with $n = 2$, 3, or 4; P−P = dppp and S−S = $S(CH_2)_4S$; P−P = 1,4-bis(diphenylphosphino)butane and S−S = $S(CH_2)_4S$;[27] the homobimetallic bridged dithiolate rhodium−rhodium complexes of general formula $[Rh_2(COD)_2\{\mu\text{-}(S-S)\}]$, where S−S = $S(CH_2)_nS$ with $n = 2$, 3;[28] and a Pt_3 trinuclear complex with two bridging S_2N_2CPh ligands.[32]

The $[SCH_2SCH_2S]^{2-}$ ligand in complex **11** resembles closely the $[SCH_2CH_2CH_2S]^{2-}$ ligand in the previously reported Pd−Rh complex,[27] with the obvious differences in bond lengths (S−C longer than C−C) and angles (C−S−C smaller than C−C−C) produced when the central CH_2 is replaced by S.

Concluding Remarks

A detailed study of the reaction of $[(P\cap P)Pt(\mu\text{-}S)_2Pt(P\cap P)]$, P∩P = dppp or dppe, with CH_2Cl_2 confirms the high nucleophilicity of the sulfide ligand in the $\{Pt_2S_2\}$ core. The experimental results have allowed us to formulate all the steps involved from the initial to the final products. In addition, they show that the nucleophilic behavior is highly dependent on the diphosphine nature. Thus, the $[Pt(dppp)(S_2CH_2)]$ complex reacts further with CH_2Cl_2 and itself to form $[Pt_2(dppp)_2\{\mu\text{-}(SCH_2SCH_2S)\text{-}S,S'\}]Cl_2$ while the dppe analogue does not. Theoretical calculations are consistent with the experimental results showing that complexes with dppp are more nucleophilic than the parent dppe compounds. This enhanced nucleophilicity can be due to a more efficient electron donation from the phosphorus lone pairs of dppp, compared to those from dppe, and it is reasonable to attribute it to the closeness of the bite angle of the dppp ligand to the P−Pt−P angle found in complexes with unidentate unconstrained phosphines. The bite angle also influences the kinetic stability of the different species formed along the reaction. The dppp ligand appears to be more flexible than dppe, and thus, it can better accommodate to the changes in the bite angle required along the reaction pathway. As a consequence, the evolution from $[(P\cap P)Pt(\mu\text{-}S)_2Pt(P\cap P)]$ to $[Pt(P\cap P)(S_2CH_2)]$ and $[Pt[(P\cap P)Cl_2]$ proceeds faster for dppe than for dppp containing complexes. Overall, the observed dependence on the nature of the ligands bound to the $\{Pt_2S_2\}$ core, together with the high number and different nature of the species characterized in this work, gives a reason for the diversity of the compounds reported in the literature as a result of the reaction of $[L_2Pt(\mu\text{-}S)_2PtL_2]$ with weak electrophilic agents.

Acknowledgment. Financial support from the Ministerio de Ciencia y Tecnología of Spain (DGICYT: BQU2001-

(32) Banister, A. J.; Gorrell, I. B.; Lawrence, S. E.; Lehmann, C. W.; May, I.; Tate, Cr.; Blake, A. J.; Rawson, J. M. *Chem. Commun.* **1994**, 1779.

1976 and PB98-0916-CO2-01) and from EPSRC (U.K.) is gratefully acknowledged. C.M. thanks the EU and CESCA/CEPBA for sponsoring her visit to the UAB under the Improving Human Potential Program, Access to Large Scale Facilities (HPRI-1999-CT-00071).

Supporting Information Available: Crystallographic files in CIF format. This material is available free of charge via the Internet at http://pubs.acs.org.

IC0107173